

## **CHAPTER 3 : BENCH-SCALE TRIBOELECTROSTATIC SEPARATOR**

### **3.1 Introduction**

Advanced techniques for coal-cleaning has been the area of research in recent years. These methods are capable of reducing ash and sulfur forming minerals from coal but have run into problems associated with the dewatering of coal. As a means of avoiding problems associated with the fine coal dewatering, the Federal Energy Technology Center (FETC) developed a dry cleaning process, in which mineral matter is separated from coal without using water. In this process, finely-sized coal is charged by means of triboelectrification and subsequently passed through an electric field for electrostatic separation. In the original idea triboelectrification was achieved by passing pulverized coal through an in-line mixer that was made of copper, whose work function was in-between, those of carbonaceous material (coal) and mineral matter. Thus, the coal particles striking on the copper wall lost electrons to the metal, thereby acquiring positive charges, while mineral matter striking on the wall gained electrons acquiring negative charges. The triboelectrostatic separation (TES) process had been tested successfully on bench-scale. The results obtained at FETC showed that it was capable of cleaning the coal of more than 90% of pyritic sulfur and 70% of the ash-forming minerals from a number of eastern U.S. coals. It was necessary however, to test the process on a proof-of-concept scale so that appropriate scale-up information could be obtained. Furthermore, it was necessary to increase the throughput of the TES process by improving the design for the electrostatic separation system.

The laboratory-scale batch TES unit used by FETC relied on adhering charged particles on parallel electrode surfaces and cleaning the electrodes. Therefore, the capacity of the TES unit was proportional to the electrode surface area. The laboratory unit could not be scaled up as such because of its low throughput and associated high maintenance. It is a well known concept that volume-based separators (eg., flotation cell etc.) have a throughput higher than surface area-based separators (magnetic drum separators (magnetic drum separators etc.).

The bench-scale continuous TES unit developed at FETC, partially overcame the difficulties associated with the laboratory scale batch TES unit. This unit separated positively and negatively charged particles splitting the gaseous stream containing these particles in an electric field by means of a flow splitter, so that the charged particles could be directed into compartments based on their charges. The two devices (bench-scale and laboratory scale) differed fundamentally in that the former was a surface area-based separator, while the latter was a volume-based separator. The bench-scale unit is referred to as an *entrained flow* separator by the in-house researchers at FETC. Thus, the entrained flow TES unit was a significant improvement over the laboratory unit with regard to throughput capacity.

As a follow-up to the work done at FETC, the current research involved designing a new TES unit which could make up for the deficiencies associated in the FETC design. In the present work, the entrained flow separator will be scaled-up to POC scale. However, a pair of circular electrodes replaced the parallel plate electrodes. There are two advantages for this type of separator. Firstly, the circular electrodes provide a non-uniform electric field (and hence, a field gradient), which may be conducive to improving the separation of oppositely charged particles from each other. Secondly, the electrodes will be rotated so that fresh surface can be exposed. This new design is similar to the open-gradient magnetic separator developed by Oak Ridge National Laboratory during the early 1980s. Therefore, the new design may be referred to as open-gradient triboelectrostatic separator. This chapter details the research objectives of this work, the design and development of the experimental set-up (containing the tribocharger and the electrostatic separator), sample preparation, results of tests conducted on different coal samples and the conclusions.

### **3.2 Research Objectives**

This research is aimed at further improving the TES process developed at FETC through bench-scale test program. The series of tests were aimed at studying the triboelectrification process and their subsequent separation. Tests were conducted on U.S. coals with an emphasis on maximizing BTU recovery and ash and sulfur rejection.

### **3.3 Description of the Bench Scale Triboelectrostatic Separator**

The Triboelectrostatic Separator unit designed and constructed as a part of this dissertation work, may be divided into two main components:

1. Feeder with the tribocharger
2. Drum Electrostatic Separator

#### ***3.3.1 Design of the Drum Electrostatic Separator***

Figure 3.1 shows a schematic representation of the bench-scale drum electrostatic separator. Coal samples were fed from a screw feeder into the charger (originally the in-line mixer, then the turbocharger). When the particles exit the charger, coal particles will charge positively while the mineral matter charges negatively. The charged particles pass through a collimator (flow straightener) and then through the uneven electric field created between two rotating circular electrodes. Positively charged coal particles were directed toward the negative electrode (which is the grounded electrode considering that potential was applied to only one electrode), while negatively charged mineral matter was directed toward the positive electrode. The flow splitter was located midway between the electrodes and was below the line of the electrodes vertically. The rotating cylindrical electrodes were self-cleaning.

Because of the cylindrical design of the electrodes, the bench-scale unit produced a non-uniform electrostatic field, which was substantially different from the uniform fields generated by previous designs that utilized flat-plate electrodes. The non-uniform field induced an additional force on the particles that varied from top to bottom of the electrodes.

### **3.4 Experimental**

#### ***3.4.1 Sample Preparation:***

During the process of collecting data, bench-scale tests were conducted on two different Pittsburgh No. 8 coal samples and one Sewell coal sample. Among the Pittsburgh coal samples, one was a run-off-mine (ROM) coal and the other, a clean coal product. Both the samples were from CONSOL Inc. The Sewell sample was from one of the AT MASSEY plant.

All the coal samples were crushed first in a jaw crusher and then in a roller mill. The crushed coal was pulverized further using a disc mill and then by a hammer mill to -140 mesh. The pulverized coal was dry-screened to obtain two different size fractions, namely: -140+200 and -200 mesh. For later tests, samples were dry-screened to different size fractions. The samples prepared as such were kept in an oven at 112<sup>0</sup>C overnight to remove the moisture from the surface of the coal particles. The sample preparation was done one day before each test program to minimize possible surface oxidation.

#### *3.4.2 Advances in the Design of tribocharger:*

An in-line mixer charger made of copper was used during the early stage of bench-scale test work. The dimensions of the mixer were 1/-inch diameter and 6 inches in length. The mixer was equipped with four blades inside the tubing, also called a Koflo design. It was soon found that at higher feed rates the mixer clogged and the separation efficiencies were low. This could possibly be attributed to excessive number of blades. It was therefore decided to run tests with a plexiglass tube without any blades inside. The use of a plexiglass tube not only eliminated the problem due to clogging but also improved the separation efficiency. Earlier work had shown that separation efficiency improved with the plexiglass due to its surface properties. The dimensions of the plexiglass charger installed as a part of the laboratory TES unit were 1-inch diameter and 16-inch in length.

The straight plexiglass charger was further modified and replaced by a newly designed feeder/charger system shown in Figure 3.2. The engineering guidelines for the design of this new charger were based on the results obtained from the tribocharger tests (conducted as a part of this project but not as a part of this dissertation) which can be summarized as follows:

- Maximizing air velocity to obtain an optimum charge difference between coal and mineral matters without causing flow disturbance within the separator.
- Maximizing wall-particle and particle-particle collision to ensure coal particles and mineral matters are charged properly.

An efficient feeding mechanism would, i) increase separation efficiency, ii) maximize the throughput of the TES unit, and iii) eliminate the clogging problems at high feed rates with finer particles.

The most recent design of charger created tribocharges by colliding the particles in the feed against one another by means of specially designed blades in the form of an impeller, which in turn was driven by an air motor. The particles charged in the above manner were fed to a rectangular feed distributor. A series of cylindrical blocks were installed in zig-zag positions to provide a very uniform distributed flow of charged particles to the separator below. This new design was intended to provide i) maximum wall-particle and particle-particle charging mechanisms, and ii) even distribution of particles in the feed stream. The striking characteristic of this new design was that the particles in the feed stream undergo strong agitation when being fed into the impeller. Thus, this new charger was referred to as turbo charger. Under the turbulent agitation conditions provided in this new turbo charger, the inter-particle charging mechanism was expected to play as important a role as the wall-charging mechanism. This substantially increased the charge of the particles.

Also, earlier test showed that separation efficiency deteriorated when the tests were run on cold and humid days. It is possible that the poor performance was due to the surface moisture on the coal particles. The surface moisture could have probably reduced the charging ability of the particles. The importance of controlling temperature, which in turn controls the surface moisture, increased the charge density on coal particles sharply above 60<sup>0</sup>C. For this reason, a heating system was installed so that tests could be run under conditions of controlled temperature (and hence humidity). At a given feed rate, the clean coal sample was cleaned in multiple stages to establish grade vs. recovery curves. Figure 3.3 shows the flowsheet for the multiple-stages testing. Figures 3.4 and 3.5 show combustible recovery vs. ash and sulfur curves respectively, for the different charger designs used. Comparison of the curves shows the improved charging and hence separation efficiency for the turbocharger over the other charger designs used in the bench-scale TES tests.

#### 3.4.3 Establishing the Grade-Recovery Curve:

As described earlier, the tests were conducted in multiple stages shown by the flowsheet. At each stage the samples were analyzed for ash and sulfur contents. The yield

$$Y = \frac{[F - T]}{[C - T]} * 100$$

and recovery of the carbon were calculated for each stage. The cumulative yields and recoveries at the end of each stage were computed using the values obtained during the individual stages as follows:

Let 'F<sub>1</sub>' be the ash content of the sample that is fed into the separator. 'C<sub>1</sub>' and 'T<sub>1</sub>' are the ash contents in the concentrates and tailing streams. The respective carbon contents in the different samples may be given as F, C and T, where,

$$F = 100 - F_1; C = 100 - C_1; T = 100 - T_1.$$

The percentage yield of carbon, 'Y' is given by,

The stage-wise recovery of carbon in percentage 'R' is given by,

The rejection of ash in any stage is a measure of the recovery of ash in the tailing stream. The rejection 'REJ' is given by,

$$REJ = \frac{[F_1 - C_1]}{[T_1 - C_1]} * \frac{T_1}{F_1} * 100$$

The cumulative grades of the coal samples after each stage were re-calculated in terms of the stage-wise recoveries and the grades. The various plots were drawn using the values obtained through the series of steps mentioned above. A similar procedure was followed for the plots of sulfur contents. The recoveries were assumed to be the same as the ones obtained for the ash contents but the rejections were calculated independently for sulfur.

#### 3.4.4 Pittsburgh #8 Clean Coal:

A series of tests were conducted on Pittsburgh #8 clean coal using the bench-scale TES unit. Tests were conducted at varying electrode potentials at a feed rate of 4 kg/hr and varying feed rates for a fixed potential. Most of the tests were conducted with the -200 mesh fraction but one set of tests was conducted on -140+200 mesh fraction to see

$$R = Y * \frac{C}{F}$$

the effect of particle size. The following sections describe the tests conducted in detail.

*Effect of electrode potential:* It is evident from the results that the TES process is capable of producing very clean products in the first stage but at relatively low combustible recoveries. Since only one separator was available for the research work, feeding the reject stream containing coal particles which reported to the wrong stream, to the separator again increased the recovery. It may be noted here that in the tests conducted at 70KV the clean coal product obtained from the first stage was further cleaned to improve the product quality. Figures 3.6 and 3.7 show the ash content and sulfur contents as a function of the electrode potential. From the figures, it seems that the rejection is highest at 70kV but in reality, at this stage of testing only the sample at 70kV was recleaned.

The results given in Figures 3.8 and 3.9 show that the rejection curves shift considerably depending on the potential applied to the electrodes. The Population Balance Model developed and described in the earlier chapter too describes this phenomenon. The attractive force or repulsive force on any particle with the electrodes is a function of the potential applied to the electrodes. It appears that the electrode potential of 20KV is not strong enough to pull the charged particles toward the electrodes. The best results were obtained at 40KV. The results obtained at 70KV are slightly inferior to those obtained at 40KV, which may be attributed to inductive charging resulting in entrainment. At very high electrode potentials, particles may move so quickly toward the oppositely charged electrode that some of the adversely (or less strongly) charged particles can report to the same product stream, thereby contaminating the product quality (or shifting the grade vs. recovery curve to the right). This property cannot be explained with any theoretical background or model developed, but has been observed to occur. Literature too talks about such an occurrence.

*Effect of Feed rates:* A series of tests were conducted on the Pittsburgh No 8 clean coal sample (-140 mesh) using the bench-scale TES unit. Tests were conducted with the positive electrode at 50KV, while varying the feed rate from 3.6kg/hr to 40.0 kg/hr. As shown, the single stage (rougher) cleaning reduced the ash contents to the 3.5-4.0% level and the pyritic sulfur contents to the 0.29% - 0.45% level, which are excellent. However only 46-47% of the combustible material could be recovered. Figures 3.10 and 3.11 compare the combustible recoveries vs. ash and combustible recoveries vs. total sulfur curves respectively. Figure 3.12 shows the pyritic sulfur rejection. These results are

comparable to those reported by the in-house work at FETC conducted using a TES unit with plate electrodes. It must however be noted that the samples used in this series of tests had considerably different feed assays that are in the range of 4.9-6.3% ash and 1.5-1.7% sulfur. Therefore, the product grade was normalized with respect to the feed grade, and plotted as shown in Figure 3.13 and 3.14. The results show that the separation efficiency of the bench-scale TES unit improves with increasing feed rate. This observation could be owing to the possibility that at higher feed rates particles acquire higher charges. It is possible that higher the feed rate to the turbocharger, the higher the number of inter-particle collisions, which in turn gives rise to higher surface charge on the particles. However at a feed rate of 31.8 kg/hr, the separation efficiency starts to deteriorate, which may be attributed to the likelihood that the energy per unit weight of feed decreased to the minimum required for efficient charging. In addition, the choke feeding (when the feeder capacity is reached in terms of the feed rate of particles) results in a decrease in the particle-wall charging mechanism, which also plays an important role in the triboelectrification mechanism.

Based on the data shown in Figures 3.15 and 3.16, combustible recovery vs. ash and sulfur rejection curves have been constructed and are presented in Figures 3.13-3.14. In each diagram, the diagonal line drawn between the top-left hand corner (100% combustible recovery) and the lower right hand corner (100% rejection) represents the zero separation efficiency. The farther a recovery vs. rejection curve is from this diagonal line, the higher the separation efficiency is.

From the combustible recovery vs. rejection curves given in Figures 3.15 and 3.16, the maximum separation efficiencies have been obtained and plotted in Figure 3.17 as a function of feed rate. As shown, the separation efficiency was low at 3.6 kg/hr, which may be attributed to the difficulty in charging the particles at a low feed rate. However, at feed rates above approximately 8.4 kg/hr, the separation efficiency remained more or less constant until the feed rate reached approximately 30 kg/hr. The separation efficiency deteriorated significantly above this limit. Thus, the maximum throughput of this bench-scale TES unit is approximately 30 kg/hr.

The Population Balance Model talks of the separation efficiency being a function of velocity in the vertical direction. The velocity in the vertically downward direction is



itself dependent on the feed rate of the particles to the feeder. Higher the feed rate, higher the velocity of particles. This increases the separation efficiency but at very high feed rates (in this case, beyond 30kg/hr), the velocity drops because of feeder capacity. So the efficiency too drops.

#### 3.4.5 Sewell Seam Clean Coal:

*Effect of Electrode Potential:* A series of tests were conducted on the Sewell seam clean coal sample (-140 mesh, 6.7% ash and 0.97% sulfur) using the bench-scale TES unit. Tests under this category were conducted at a feed rate of 8.2 kg/hr, while varying the applied electrode voltages in four steps, namely +30, +40, +50, +60 kV. At a given potential, the coal sample was cleaned in multiple stages as shown in the flowsheet to establish grade vs. recovery curves as before.

Figures 3.18 and 3.19 show the combustible recovery vs. ash and the combustible recovery vs. total sulfur curves, respectively. The results show that the best separation efficiency of the TES unit on Sewell seam sample was obtained at 40 and 50 kV. When the potential was increased beyond 50kV or decreased below 40kV, the performance deteriorated. It is understood from previous work and tests conducted on various samples that, in a strong electric field, the particle charge may be altered due to entrainment, which is detrimental to the separation process. Based on data shown in Figures 3.18 and 3.19, the ash and total sulfur rejection curves are plotted in Figures 3.20 and 3.21. The curves show that the ash rejection pattern for Sewell seam sample is better than the total sulfur rejection pattern. This may possibly be attributed to the low inherent sulfur content of the sample.

*Behavior of different size fractions:* Figures 3.22 and 3.23 compare the combustible recovery vs. ash and combustible recovery vs. sulfur curves, respectively at different size fractions. As before the samples used in this series of tests had feed assays that are in the range of 5.43-7.31% ash and 0.99-1.04% sulfur. Therefore the product grade was normalized with respect to the feed grade, and plotted as shown in Figures 3.24 and 3.25. The results show that reasonable separation efficiencies were obtained when the coarse size fractions of the coal sample (+150 mesh) were used in the bench-scale TES unit. Separation efficiency deteriorated drastically when finer size fraction (-150 mesh) of the sample was used. Particle charging mechanism is most critically dependent on the

particle size and the velocity of air that feeds the particles to the tribocharger. Either decreasing particle size or increasing particle transport velocity can maximize the difference between the charge densities of coal and mineral matter. However, the drag force created by the turbulence at high air velocity is likely to cause the entrainment problem associated with fine particle separation, which in turn deteriorates the separation efficiency of the TES. Based on the data shown in Figures 3.24 and 3.25, combustible recovery vs. ash rejection and sulfur rejection curves were constructed and presented in Figures 3.26 and 3.27. The results show that the ash rejection was better than the total sulfur rejection with the Sewell coal tested under the conditions employed in the present work. The low sulfur rejection on this particular coal can be attributed to its low inherent sulfur content.

#### 3.4.6 Pittsburgh Run-off-mine Coal:

*Effect of Electrode Potential:* Pittsburgh No:8 ROM coal was run through series of tests wherein the electrode potential was varied in three steps, namely 20kV, 40kV and 70kV, similar results as the other two samples of coal was observed. It was observed that at 40kV, the highest separation efficiency was attained. The efficiency was low at 20kV and again at 70kV, it dropped. This particular sample was the first used in the series of tests in this research work. The sample was cleaned in multiple stages as shown in Figure 3.3 and analyzed. The sample was not used in further tests owing to the fact that the application of the bench-scale unit was in utility plants that used clean coals. Nevertheless, the clean and ROM samples behaved in a similar fashion when electrode potential was varied.

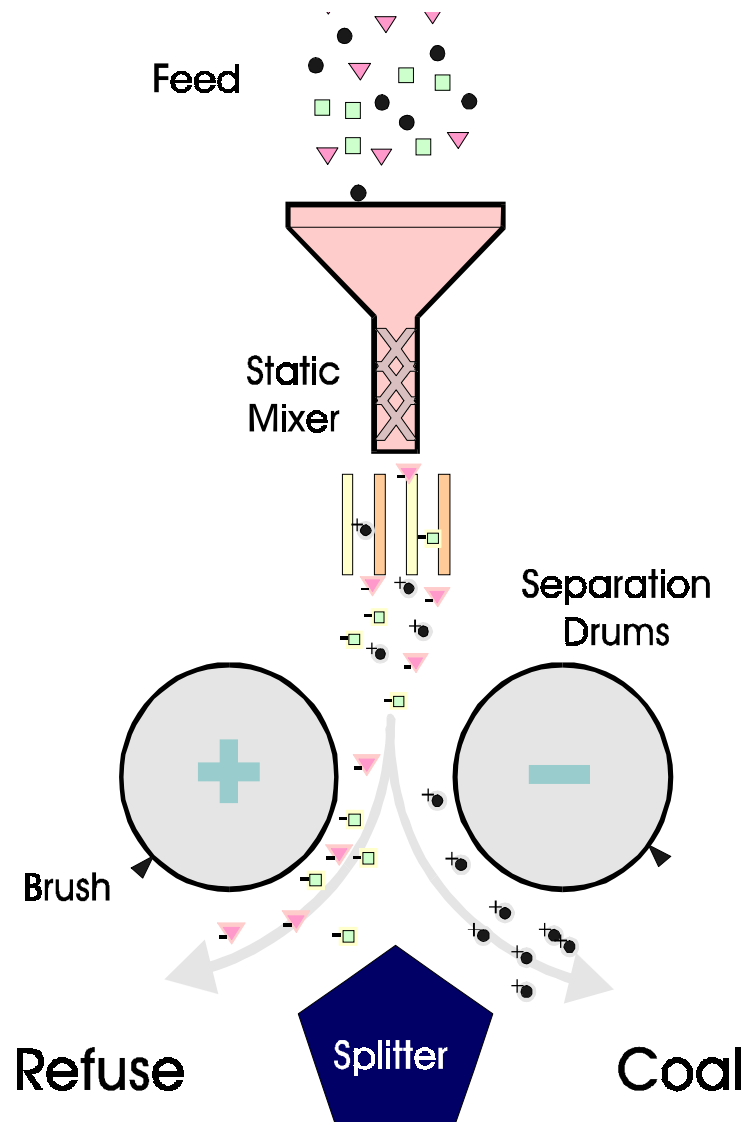


Figure 3.1 Schematic representation of the open-gradient triboelectrostatic separator used in the present work.



Figure 3.2a. Schematic representation of the tribocharger and feed distribution system used in the preliminary work.

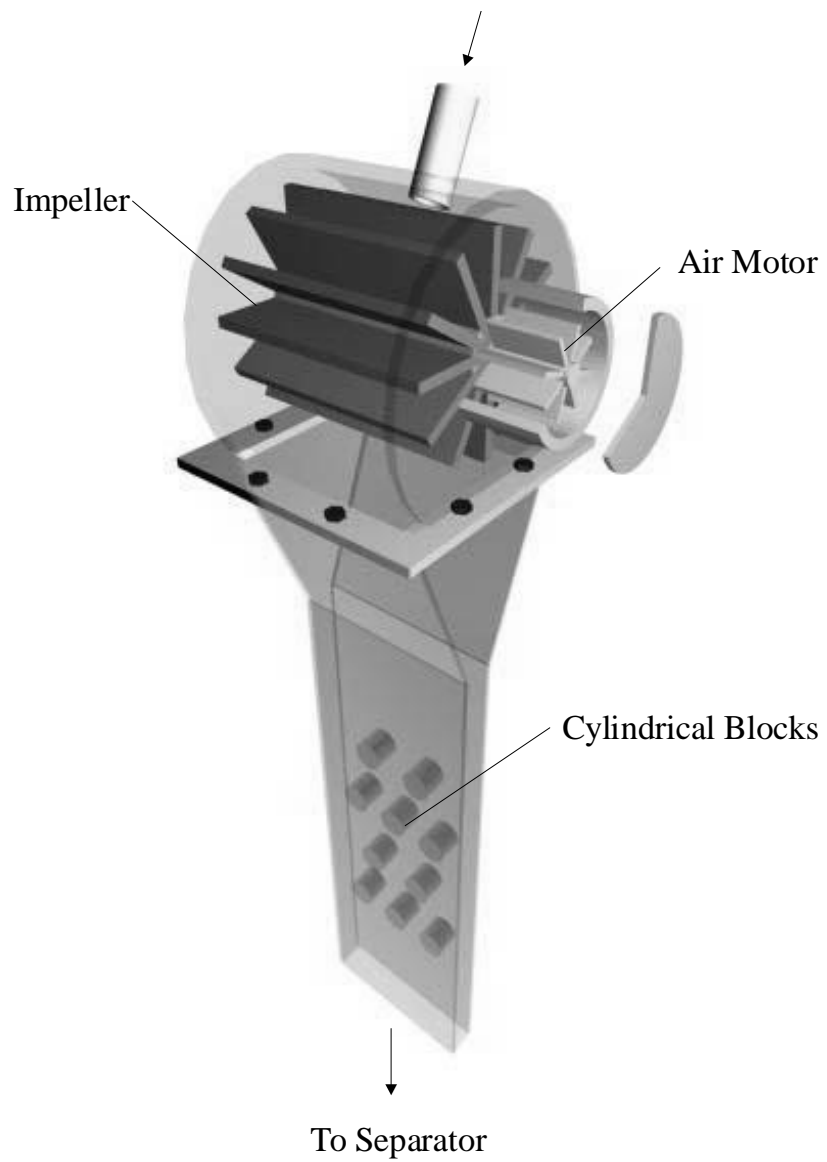


Figure 3.2b Schematic of the new turbo charger used in the TES bench-scale unit separation study.

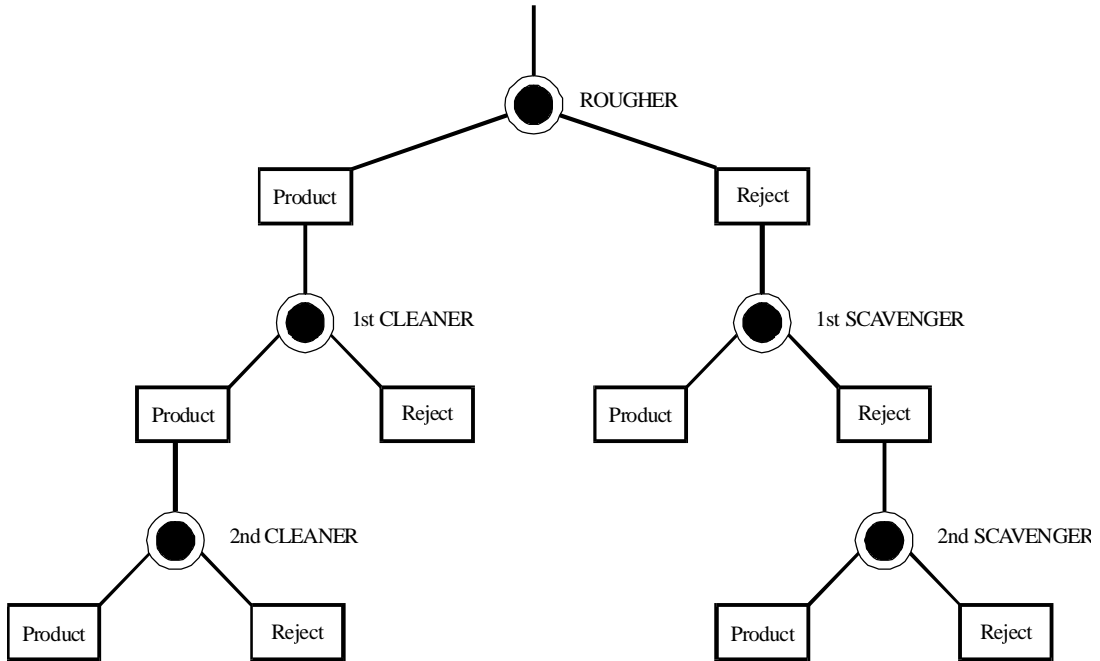


Figure 3.3 Flowsheet of the test work conducted during the course of experiments

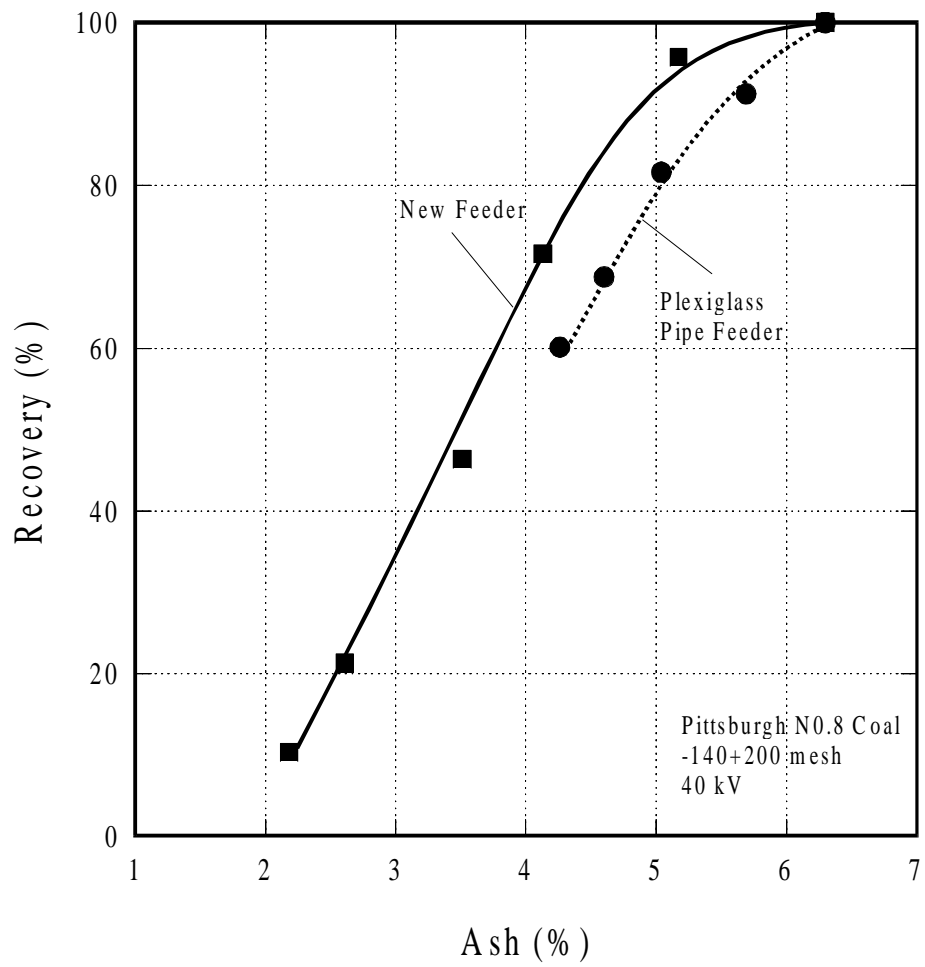


Figure 3.4 Comparison of separator efficiency in product ash content. The results were obtained on Pittsburgh No. 8 clean coal sample with different chargers installed.

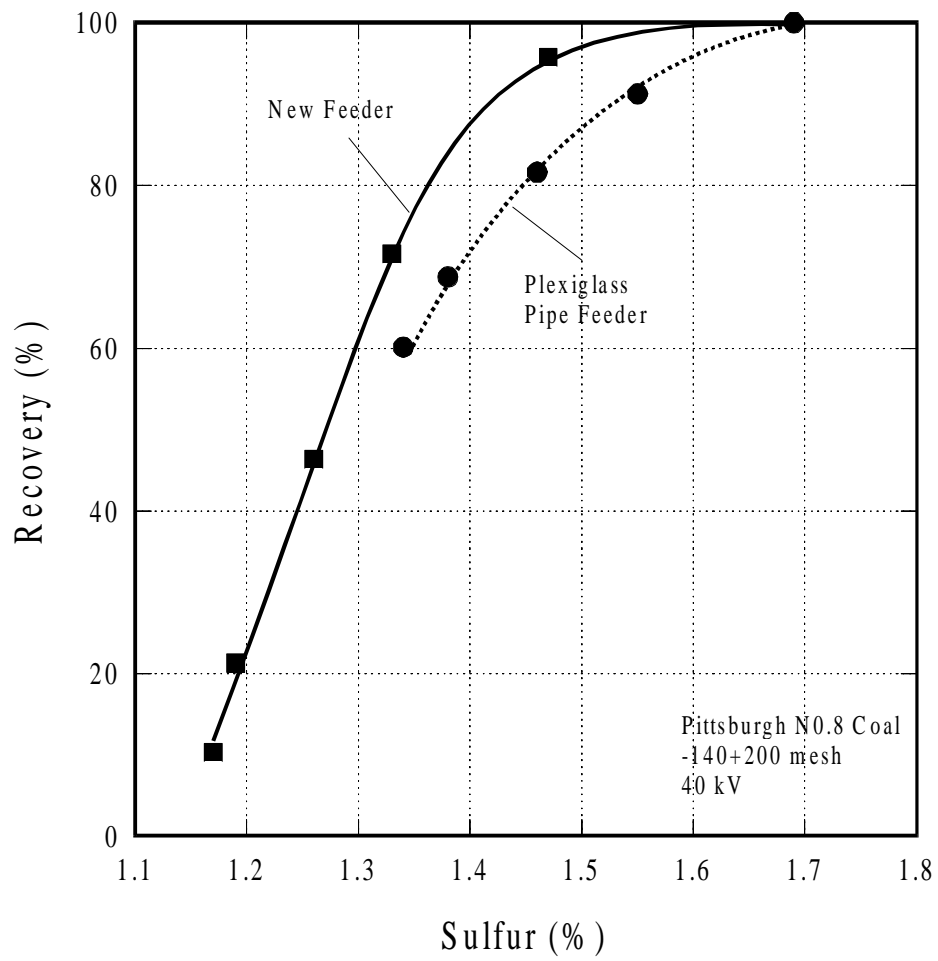


Figure 3.5 Comparison of separator efficiency in product sulfur content. The results were obtained on Pittsburgh No. 8 clean coal sample with different chargers installed.



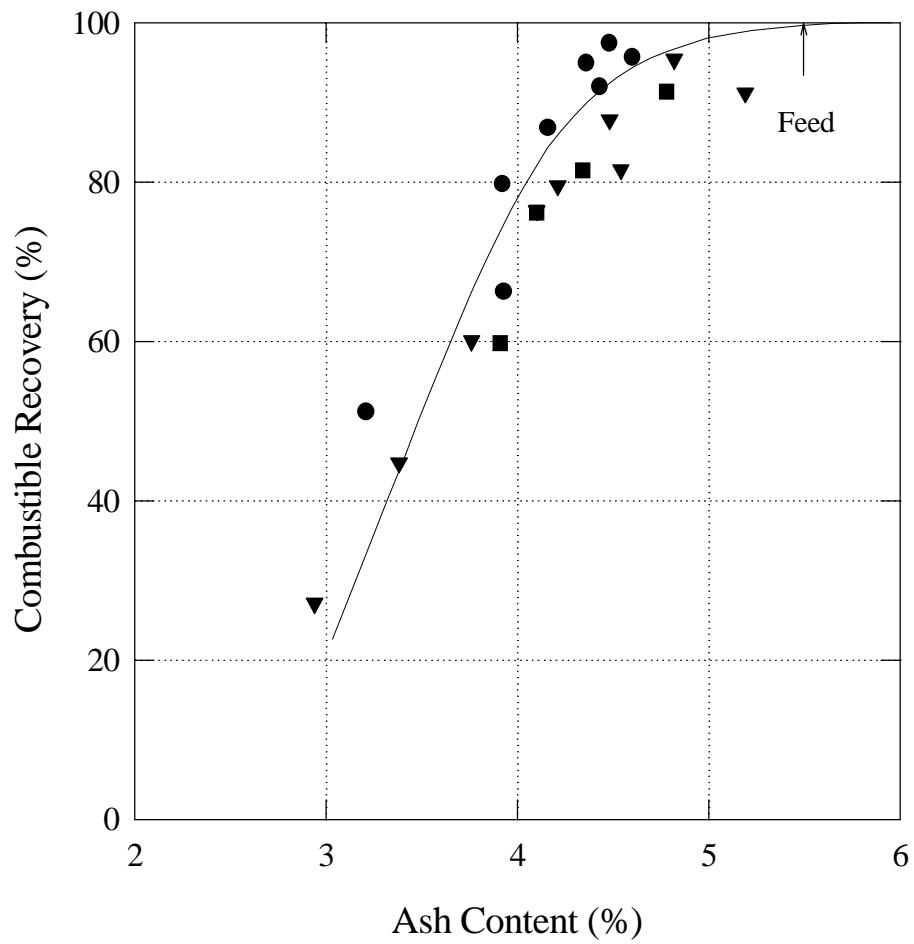


Figure 3.6 Product ash content as a function of combustible recovery. The results were obtained on Pittsburgh No. 8 clean coal sample in the TES bench-scale Unit separation study.

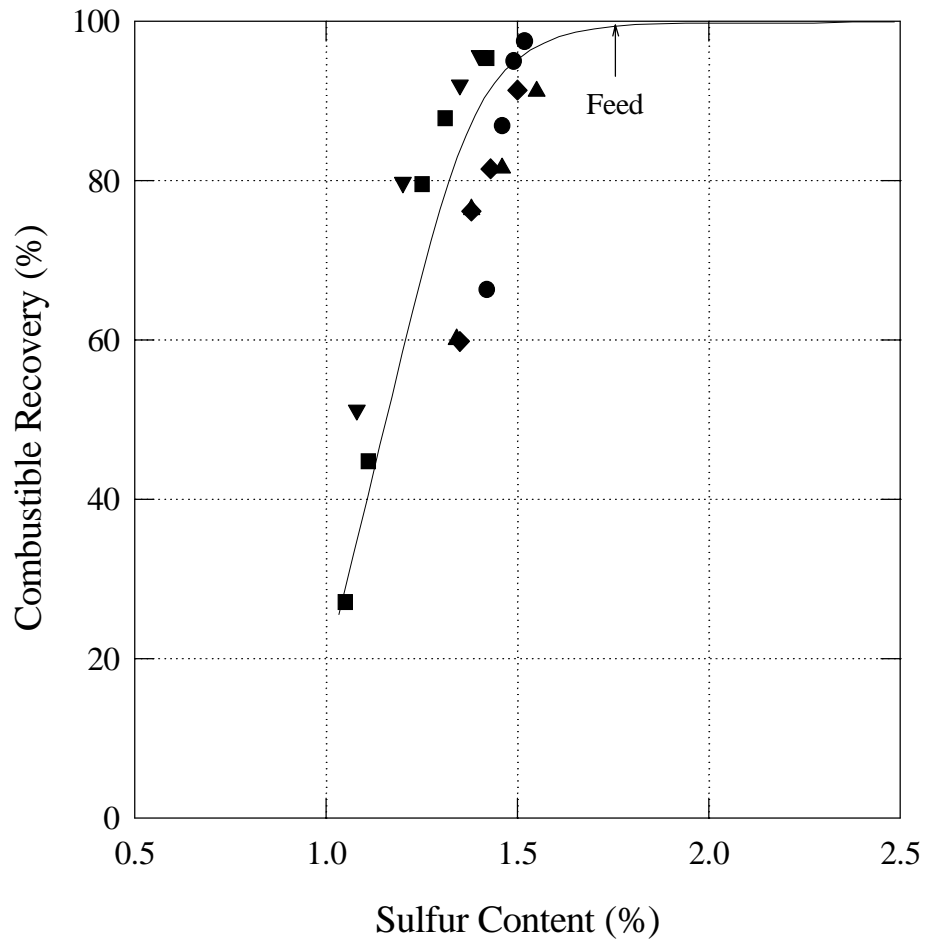


Figure 3.7 Product sulfur content as a function of combustible recovery. The results were obtained on Pittsburgh No. 8 clean coal sample in the TES bench-scale Unit separation study.

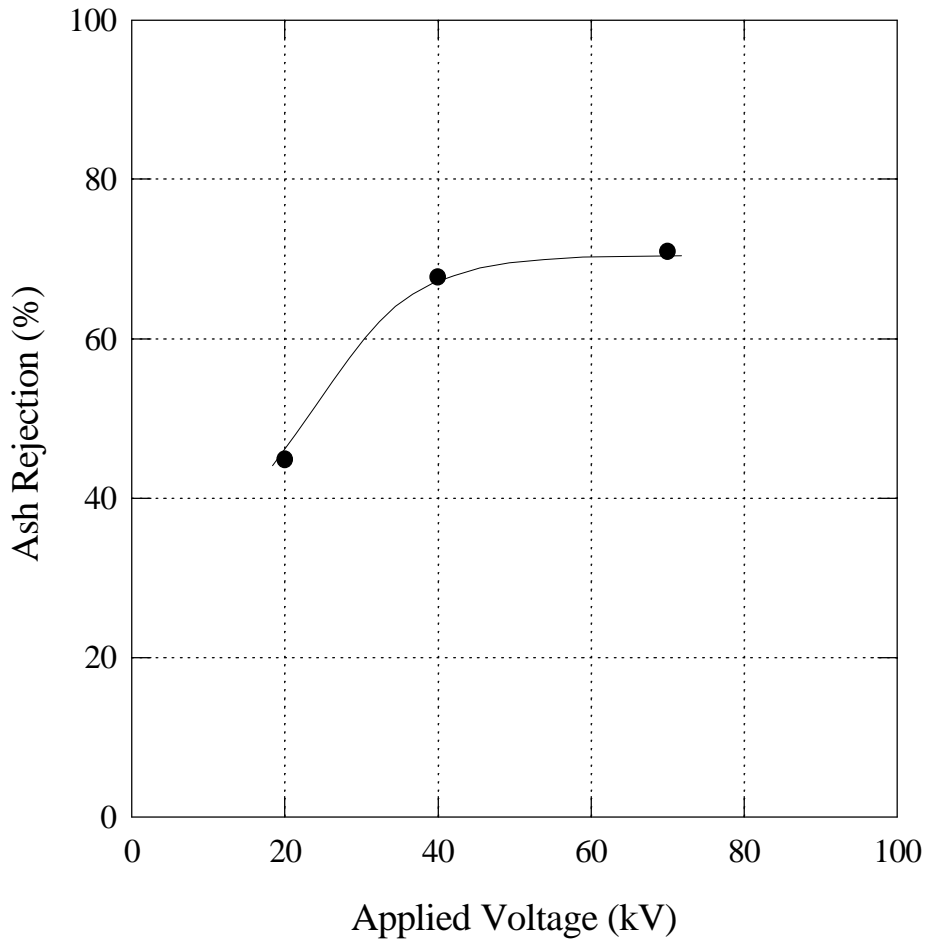


Figure 3.8 Effect of applied electrode potential on ash rejection. The results were obtained on Pittsburgh No. 8 clean coal sample in the TES bench-scale Unit separation study.

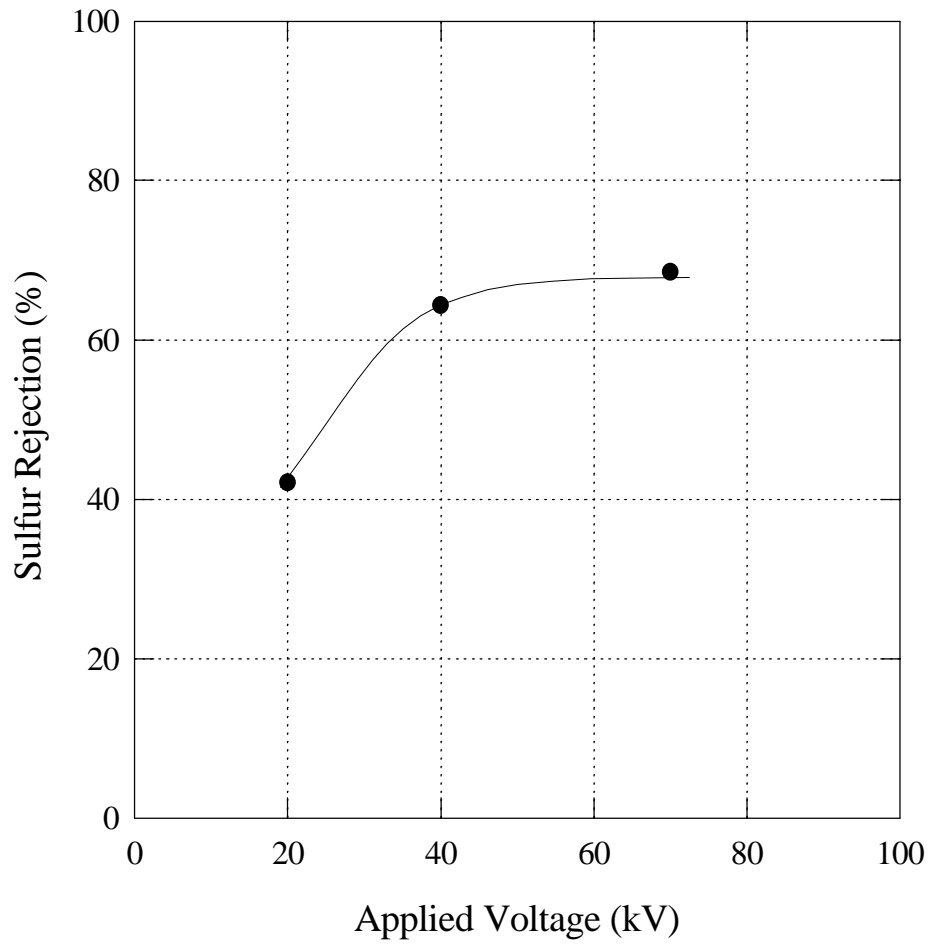


Figure 3.9 The effect of applied electrode potential on sulfur rejection. The results were obtained on Pittsburgh No. 8 clean coal sample in the TES bench-scale Unit separation study.

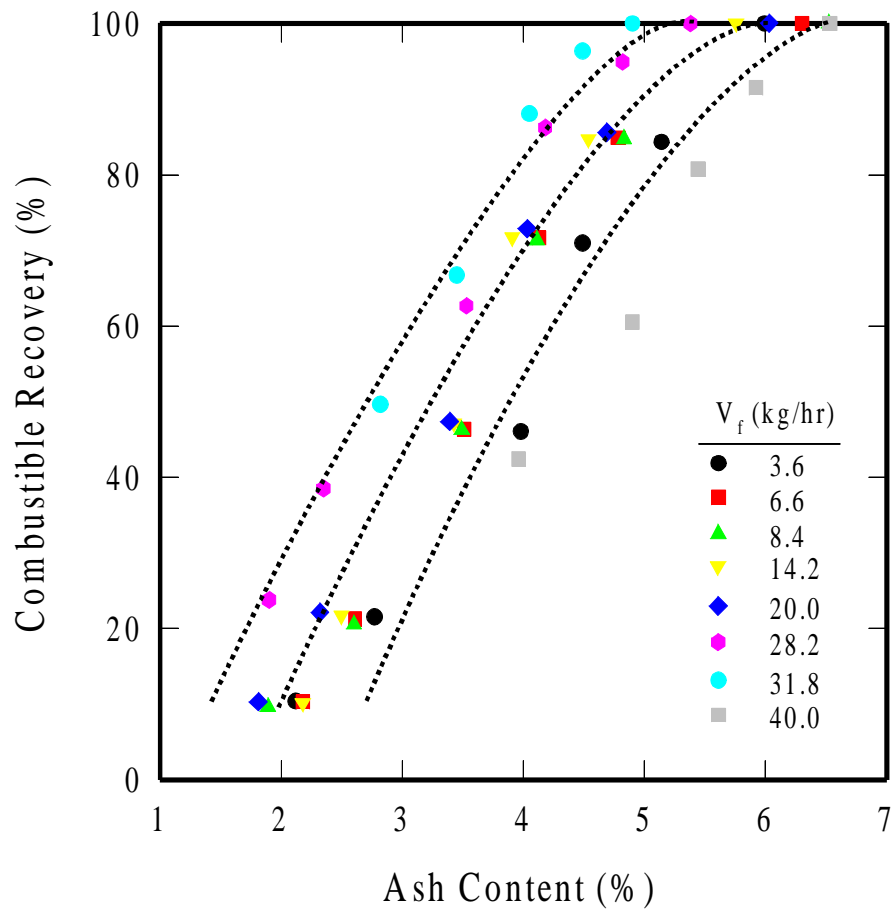


Figure 3.10 The effect of feed rate on the separation efficiency of the bench-scale TES unit. The ash vs. recovery curves were obtained on a Pittsburgh No. 8 clean coal sample with a feed rate in the range of 3.6-40.0 kg/hr.

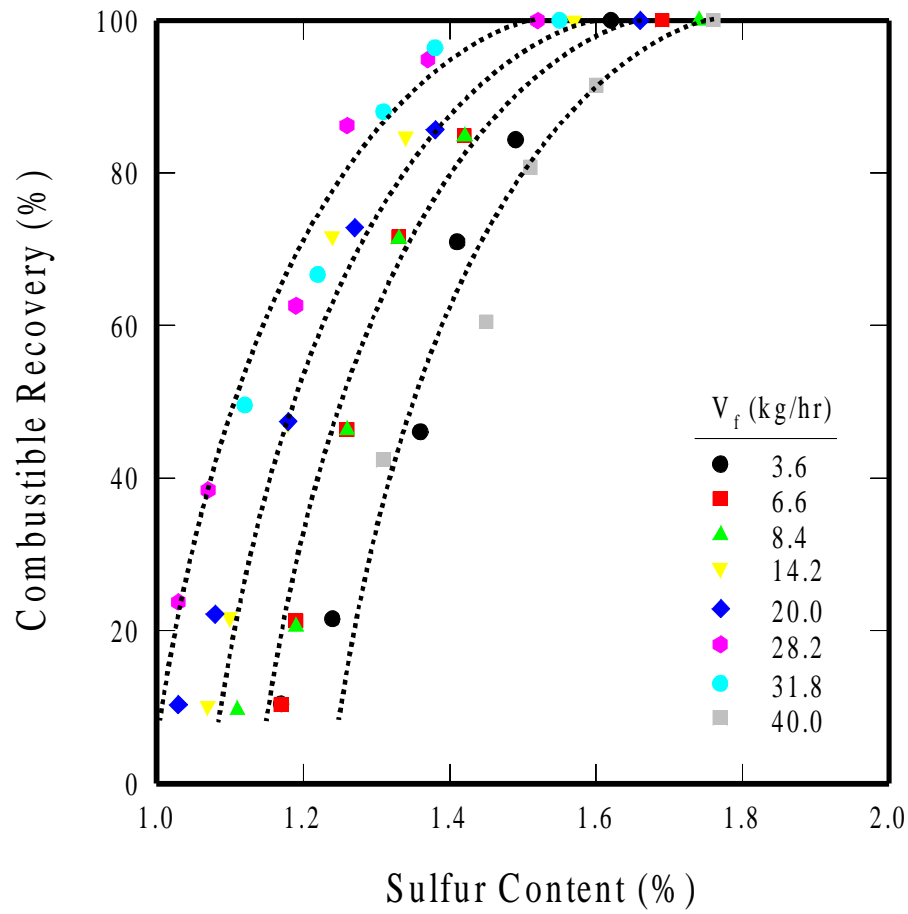


Figure 3.11 The effect of feed rate on the separation efficiency of the bench-scale TES unit. The sulfur vs. recovery curves were obtained on a Pittsburgh No. 8 clean coal sample with a feed rate in the range of 3.6– 40.0 kg/hr.

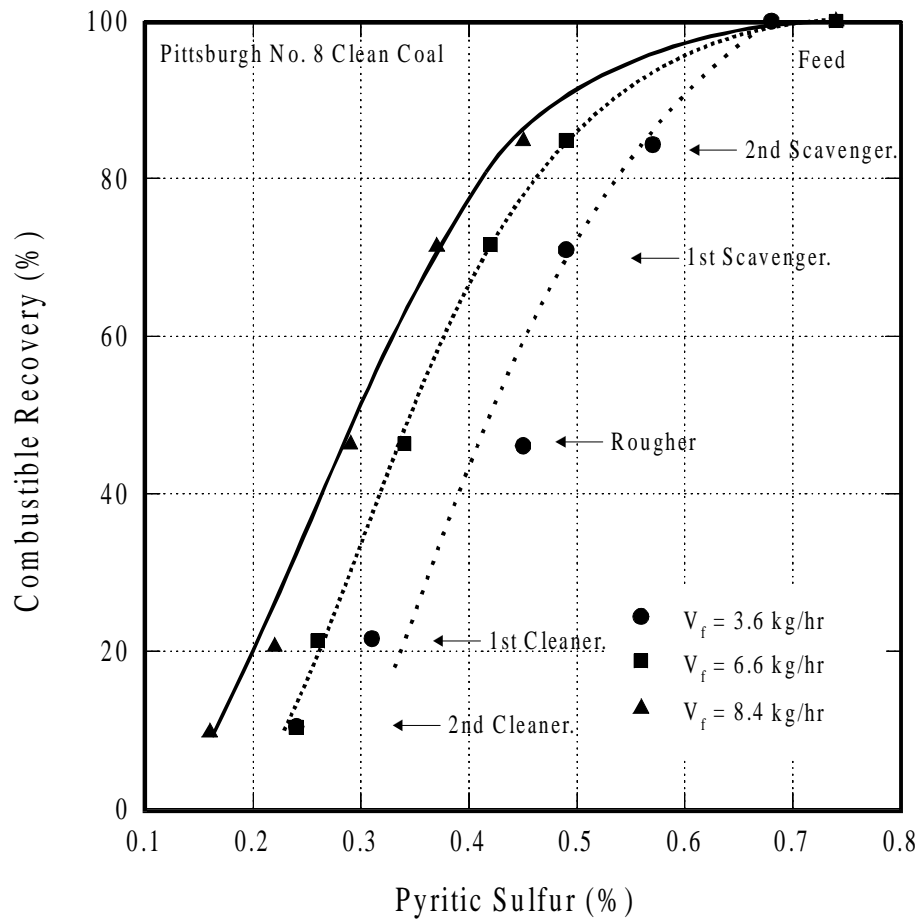


Figure 3.12 Effect of the feed rate on the TES unit separation efficiency. The grade vs. recovery curve (pyritic sulfur) were obtained on Pittsburgh No. 8 clean coal sample with varies separator feed rates.

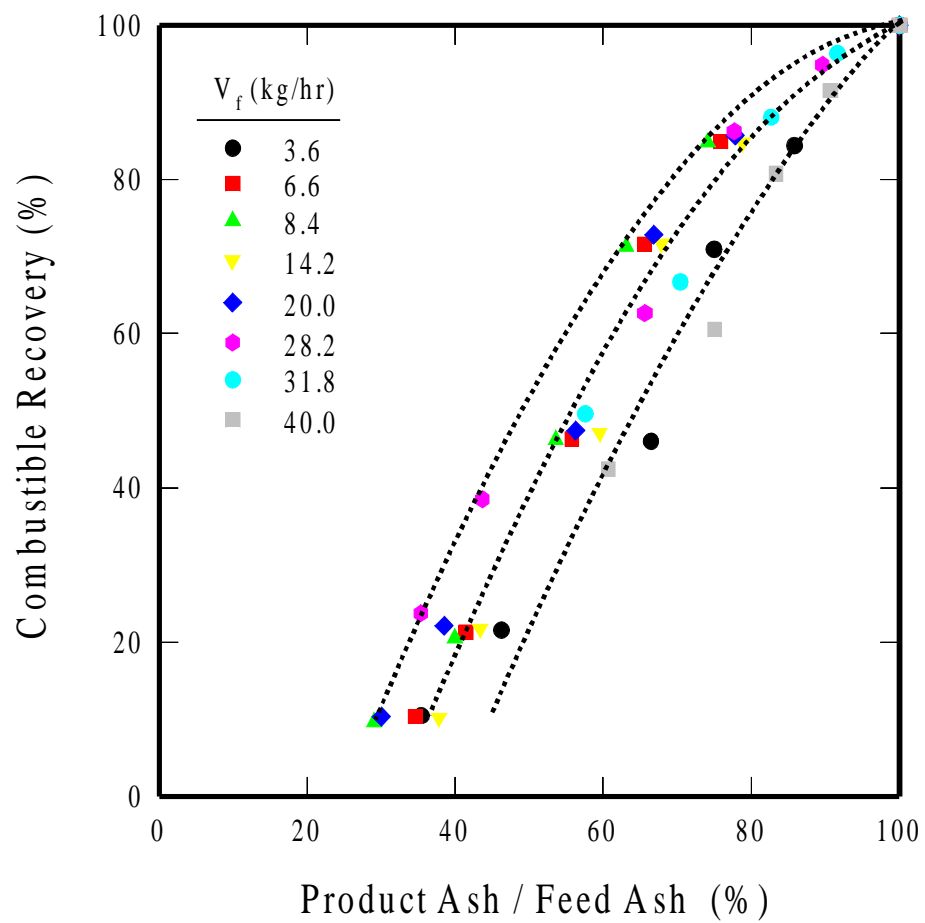


Figure 3.13 The effect of feed rate on the separation efficiency of the bench-scale TES unit. The normalized ash vs. recovery curves were obtained on a Pittsburgh No. 8 clean coal sample with a feed rate in the range of 3.6 – 40.0 kg/hr.



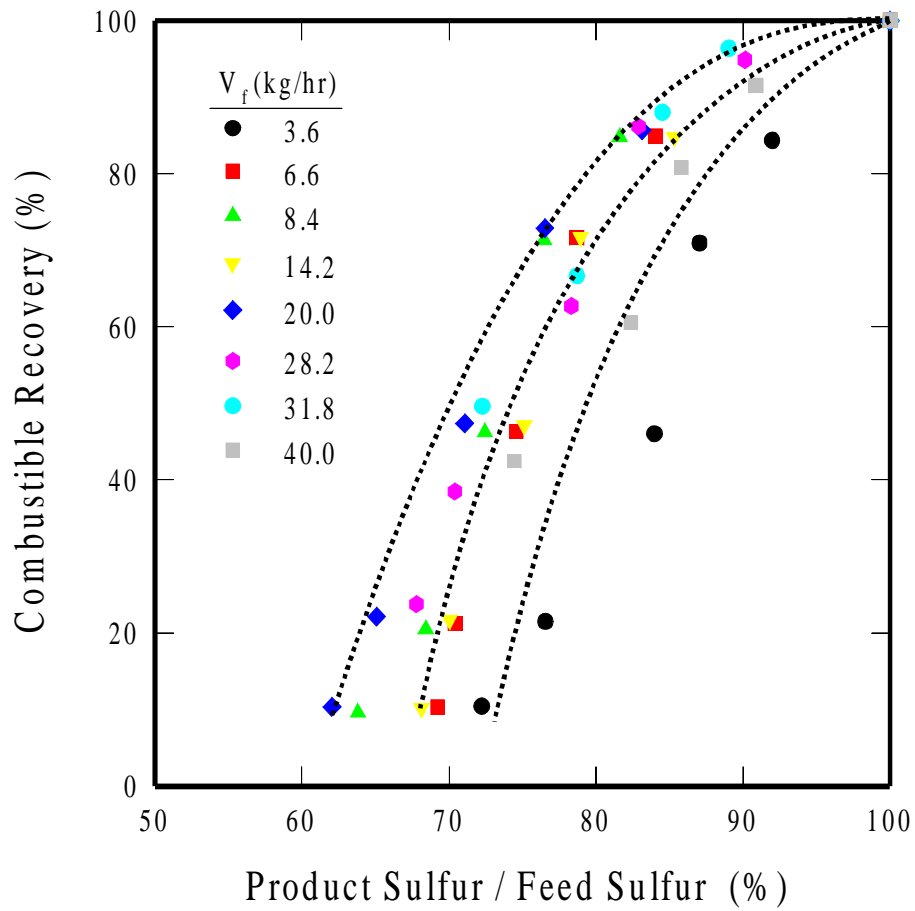


Figure 3.14 The effect of feed rate on the separation efficiency of the bench-scale TES unit. The normalized sulfur vs. recovery curves were obtained on a Pittsburgh No. 8 clean coal sample with a feed rate in the range of 3.6 – 40.0 kg/hr.

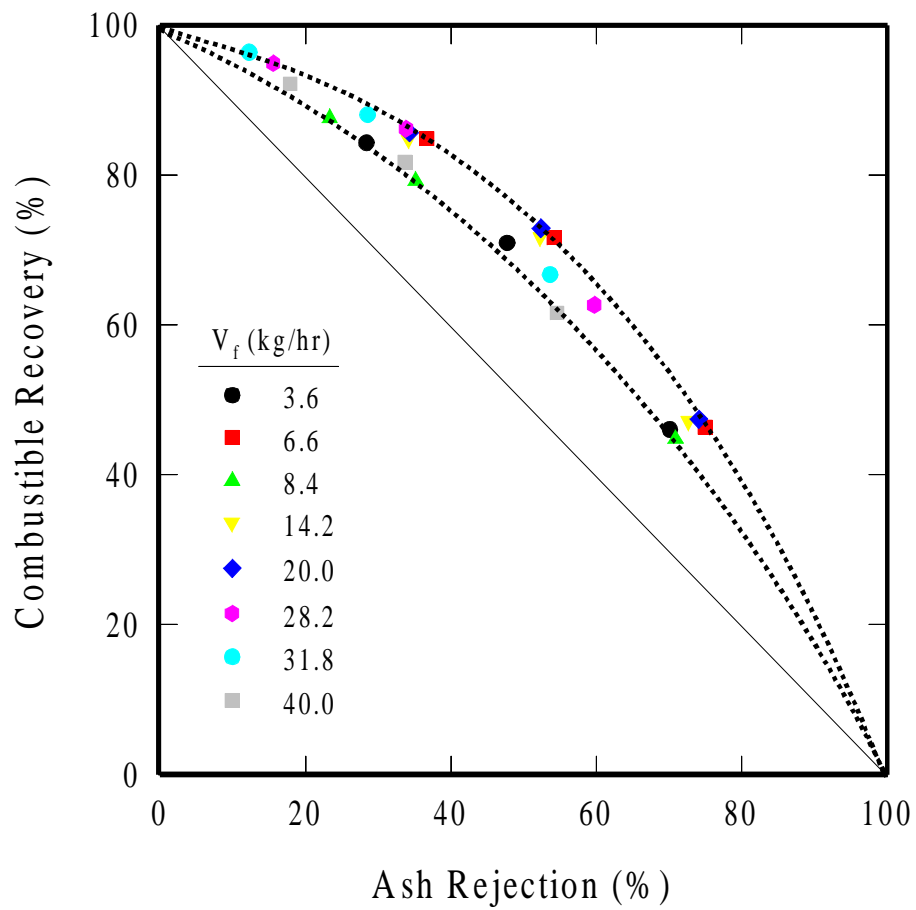


Figure 3.15 Ash rejection as a function of combustible recovery. The results were obtained on a Pittsburgh No. 8 clean coal sample in the bench-scale TES Unit study.

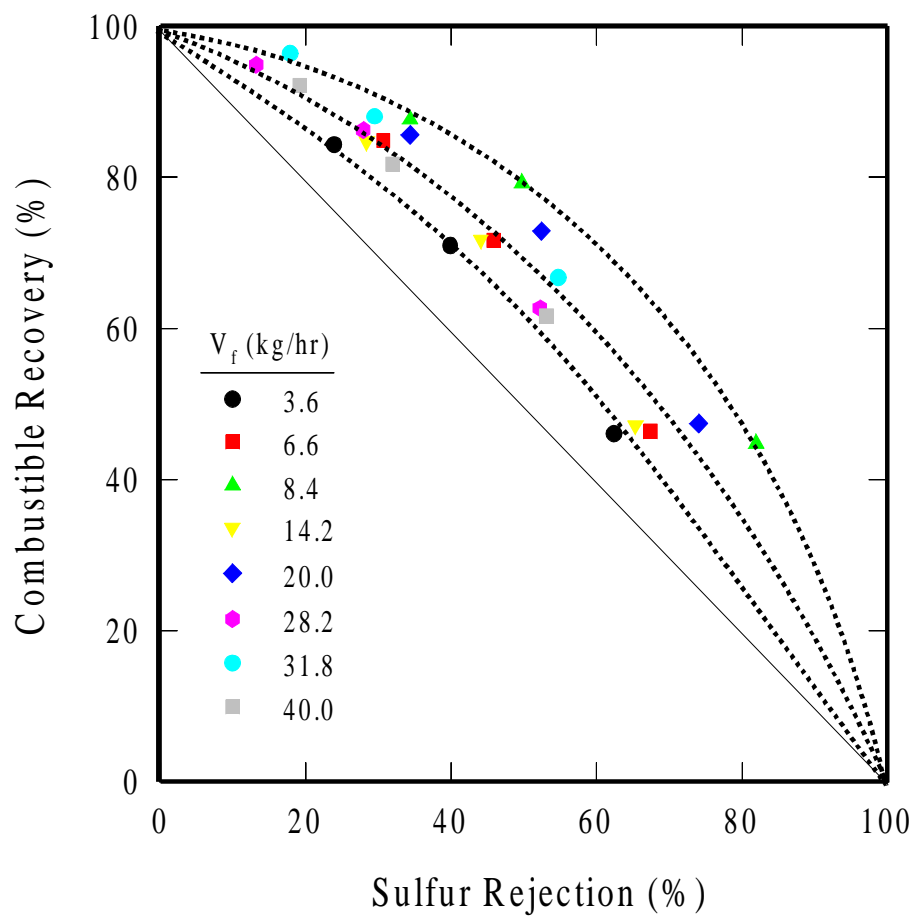


Figure 3.16 Total sulfur rejection as a function of combustible recovery. The results were obtained on Pittsburgh No. 8 clean coal sample in the TES bench-scale Unit separation study.

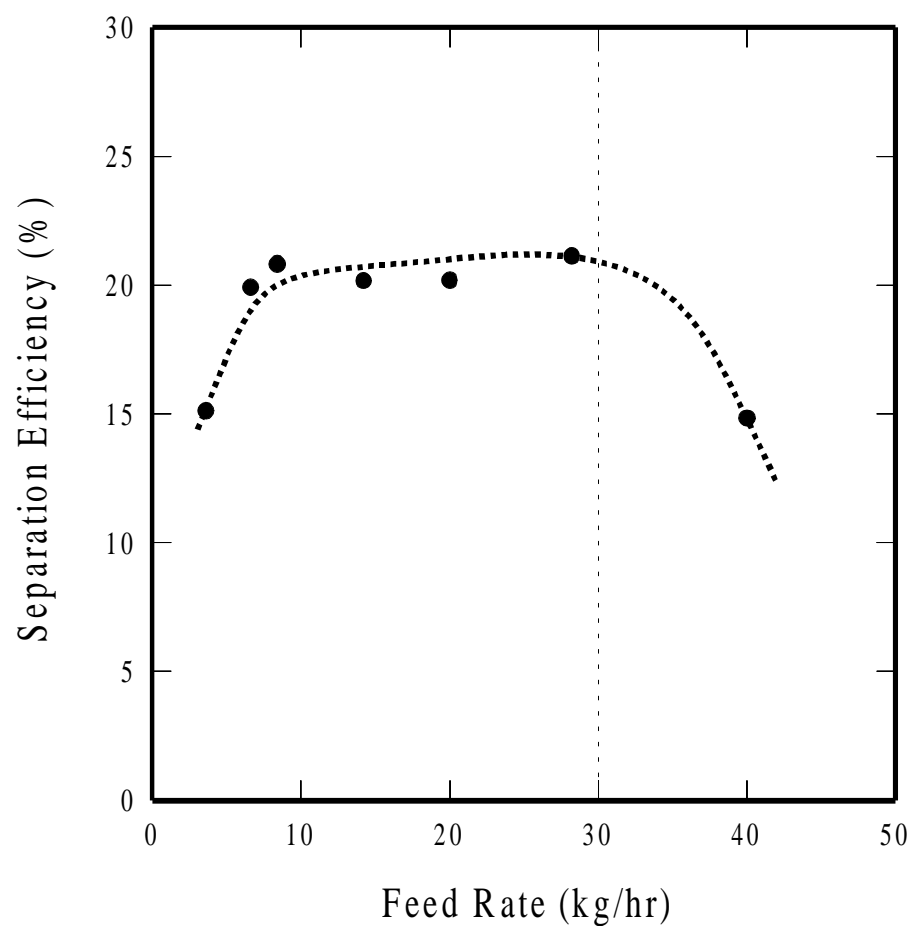


Figure 3.17 Separation efficiency as a function of feed rate. The maximum throughput of the bench-scale TES unit was found approximately 30 kg/hr.

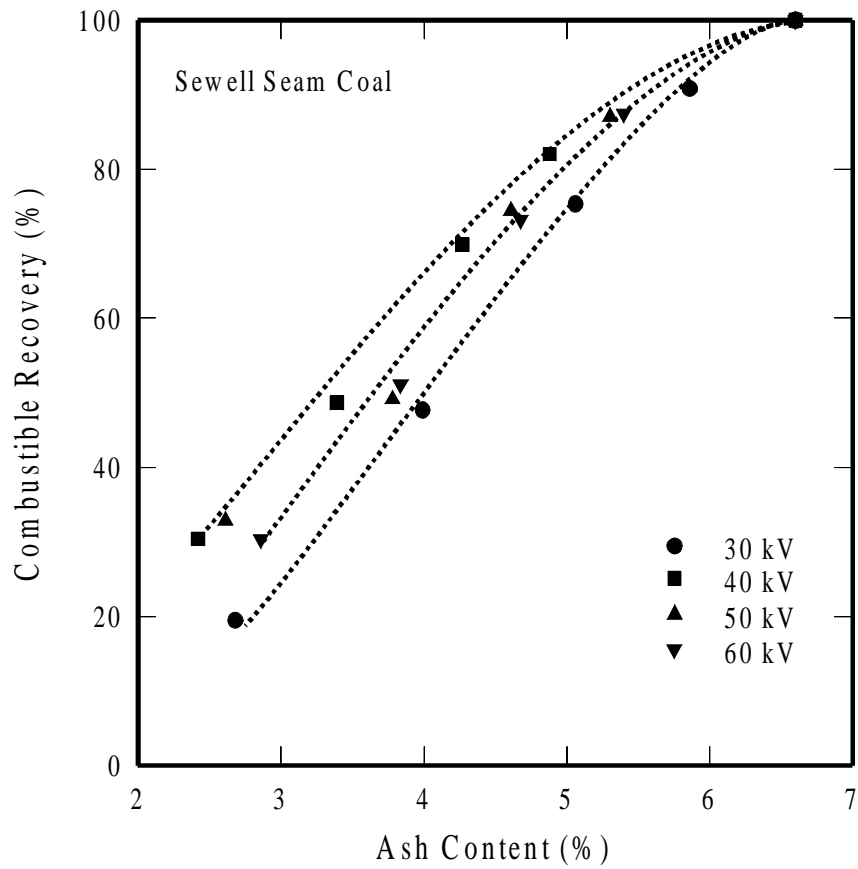


Figure 3.18 Effect of the electrical field strength on the separation efficiency of the bench-scale TES unit. The grade vs. recovery curves (ash) were obtained on a Sewell seam clean coal sample with different voltage intensities.

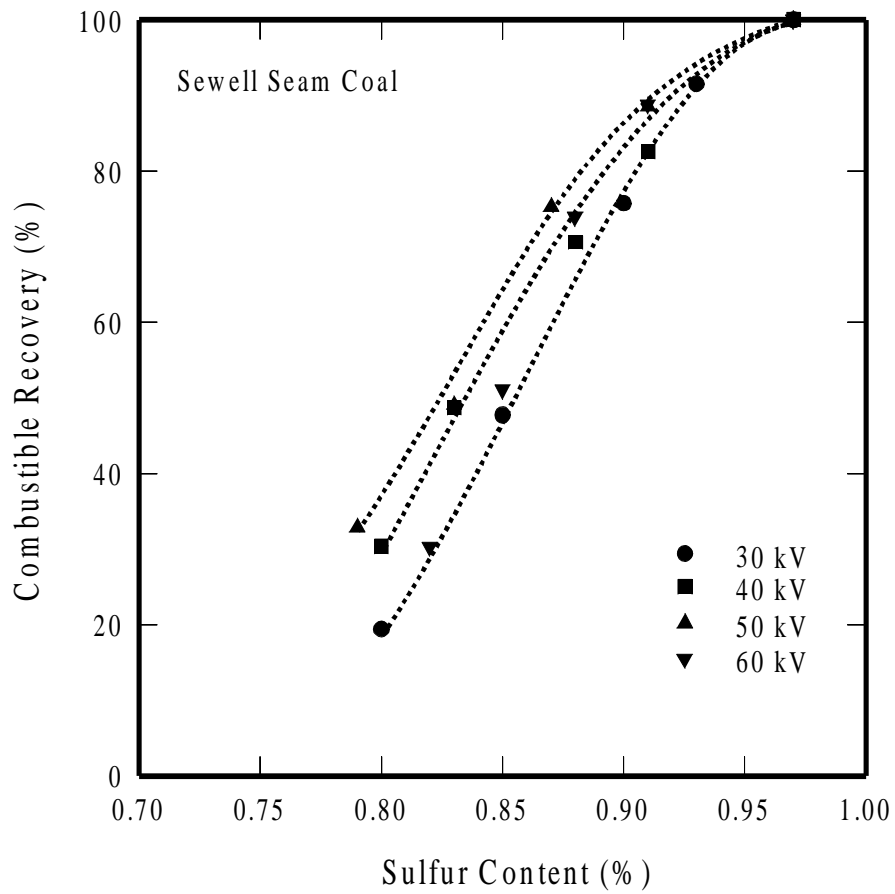


Figure 3.19 Effect of the electrical field strength on the separation efficiency of the bench-scale TES unit. The grade vs. recovery curves (sulfur) were obtained on a Sewell seam clean coal sample with different voltage intensities.

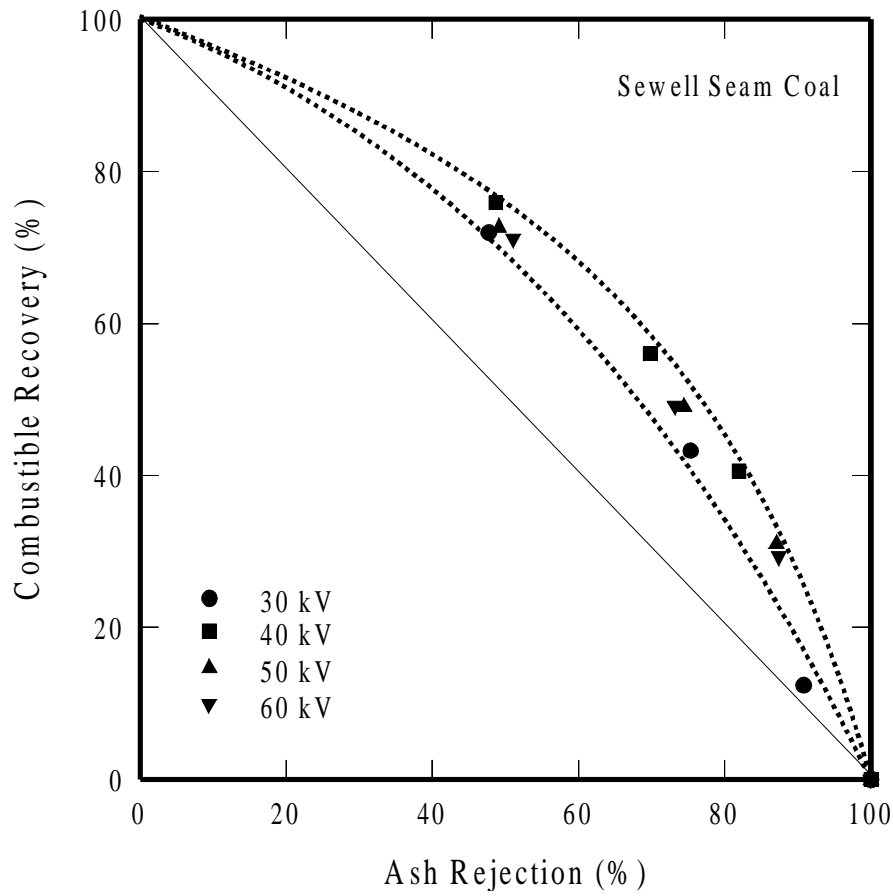


Figure 3.20 Combustible recovery as a function of ash rejection. The bench-scale TES unit test results were obtained on a Sewell seam clean coal sample in the present study.

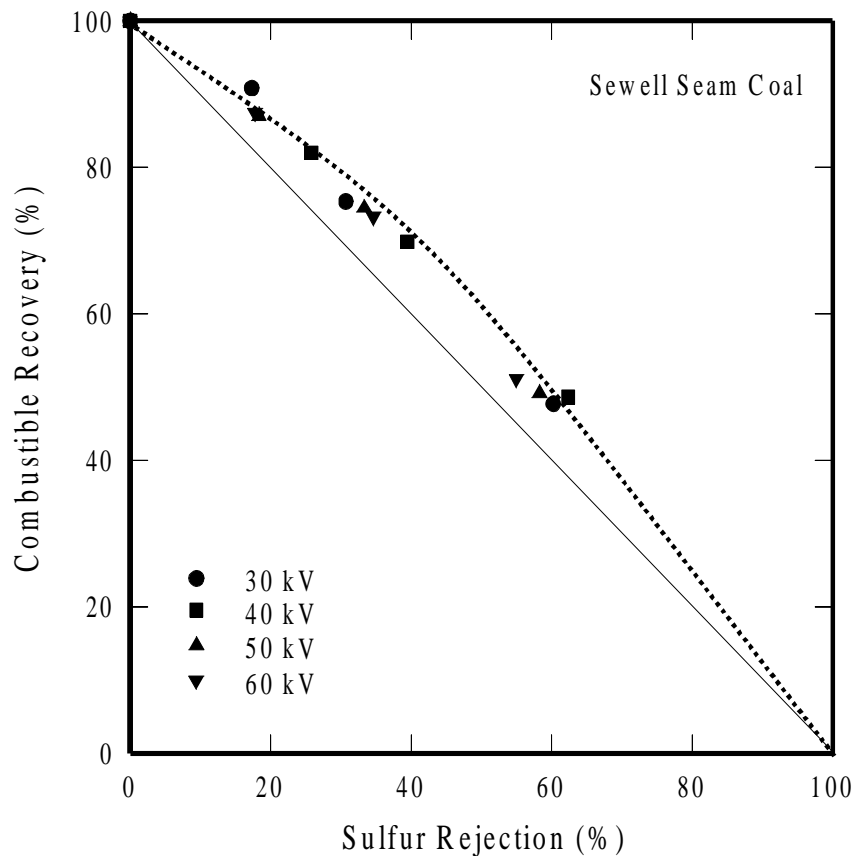


Figure 3.21 Combustible recovery as a function of total sulfur rejection. The bench-scale TES unit test results were obtained on a Sewell seam clean coal sample in the present study.



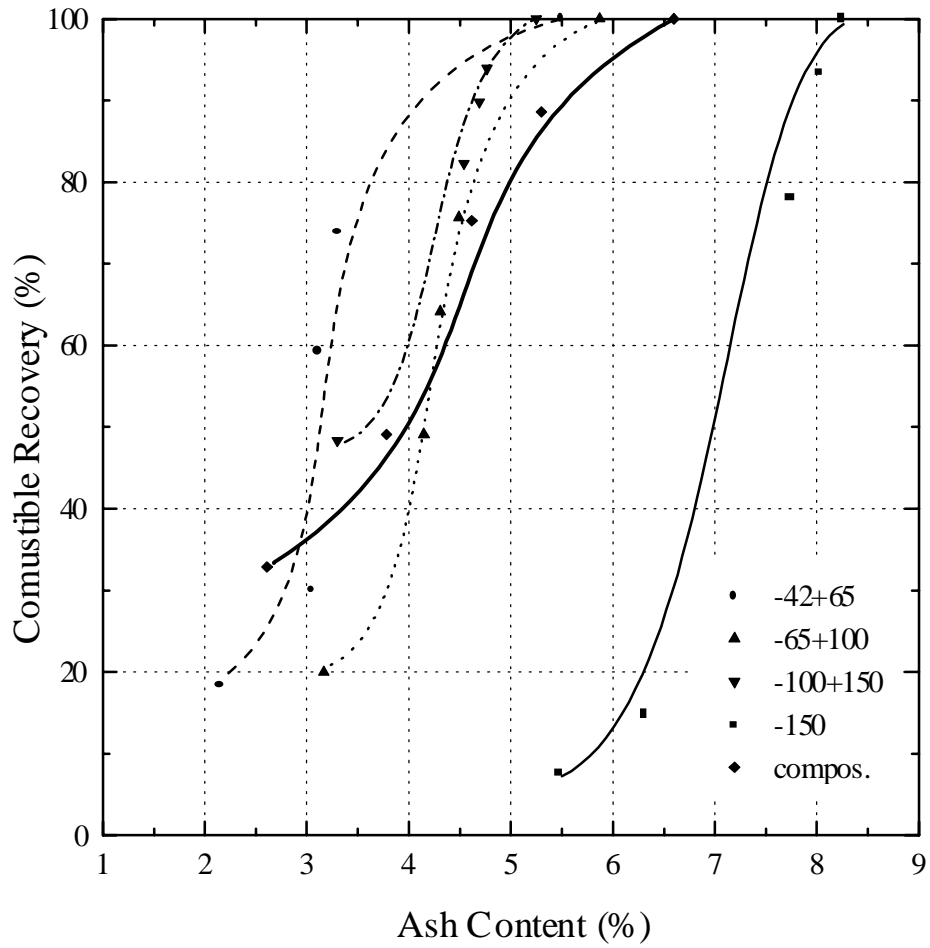


Figure 3.22. The effect of feed size on the separation efficiency of the bench-scale TES unit. The ash content vs. recovery curves were obtained on a Sewell Seam sample.

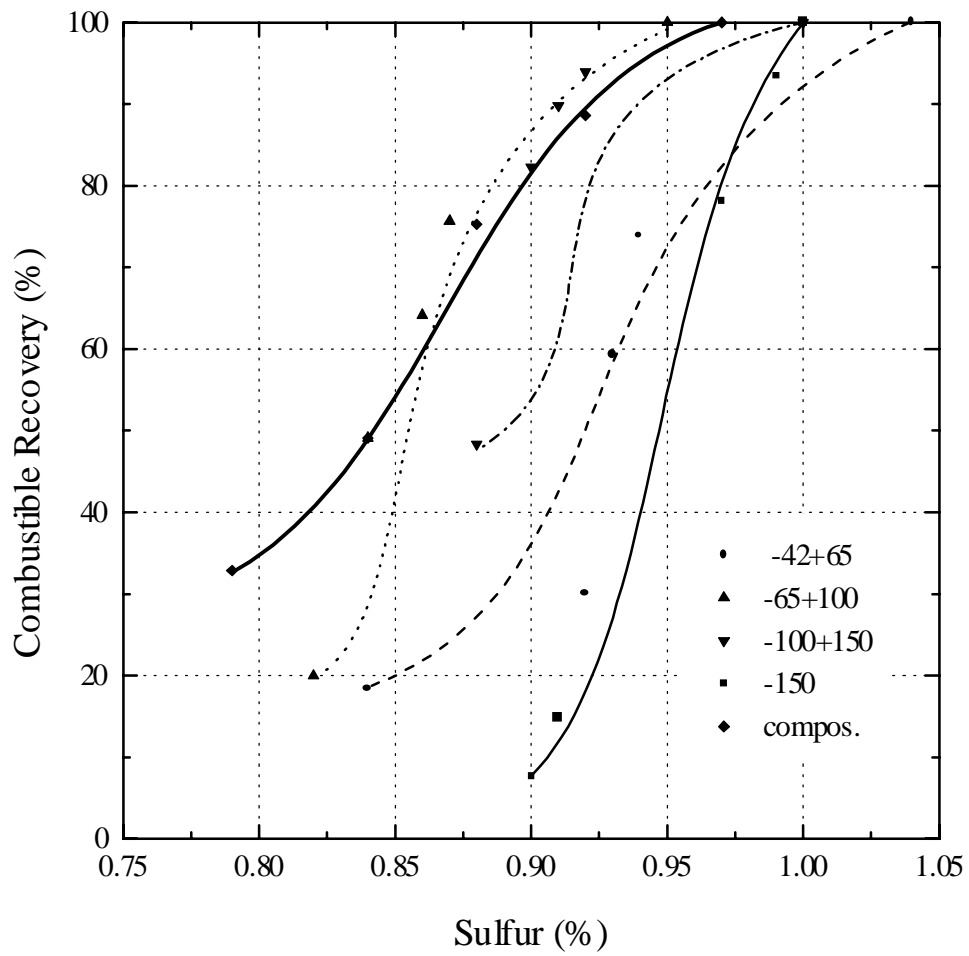


Figure 3.23. The effect of feed size on the separation efficiency of the bench-scale TES unit. The total sulfur content vs. recovery curves were obtained on a Sewell Seam sample.

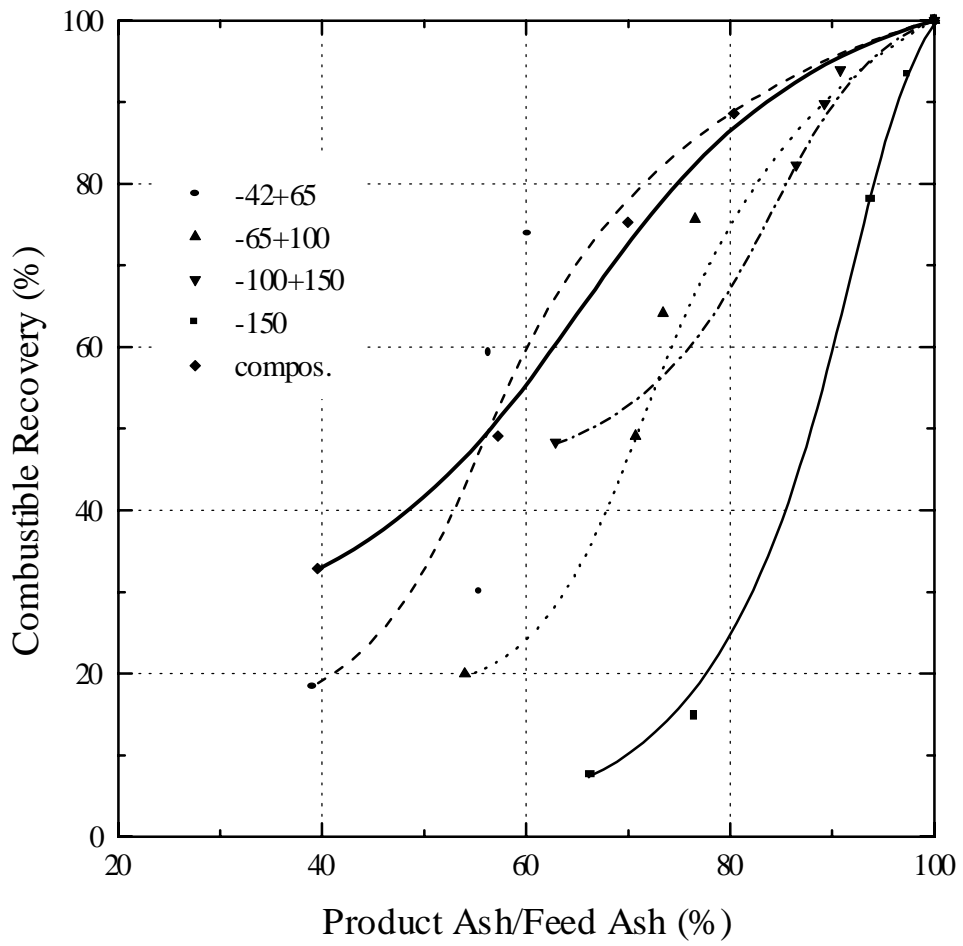


Figure 3.24 The effect of feed size on the separation efficiency of the bench-scale TES unit. The normalized ash vs. recovery curves were obtained on a Sewell Seam sample.

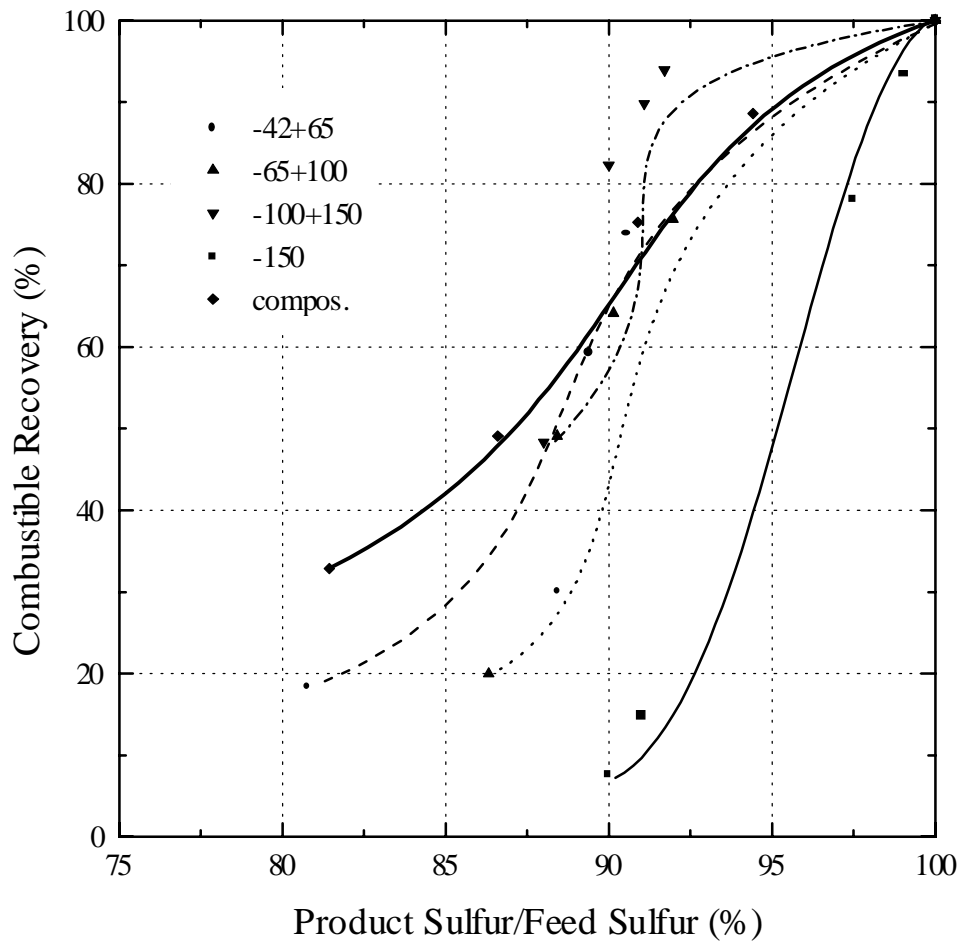


Figure 3.25. The effect of feed size on the separation efficiency of the bench-scale TES unit. The normalized sulfur vs. recovery curves were obtained on a Sewell Seam sample.

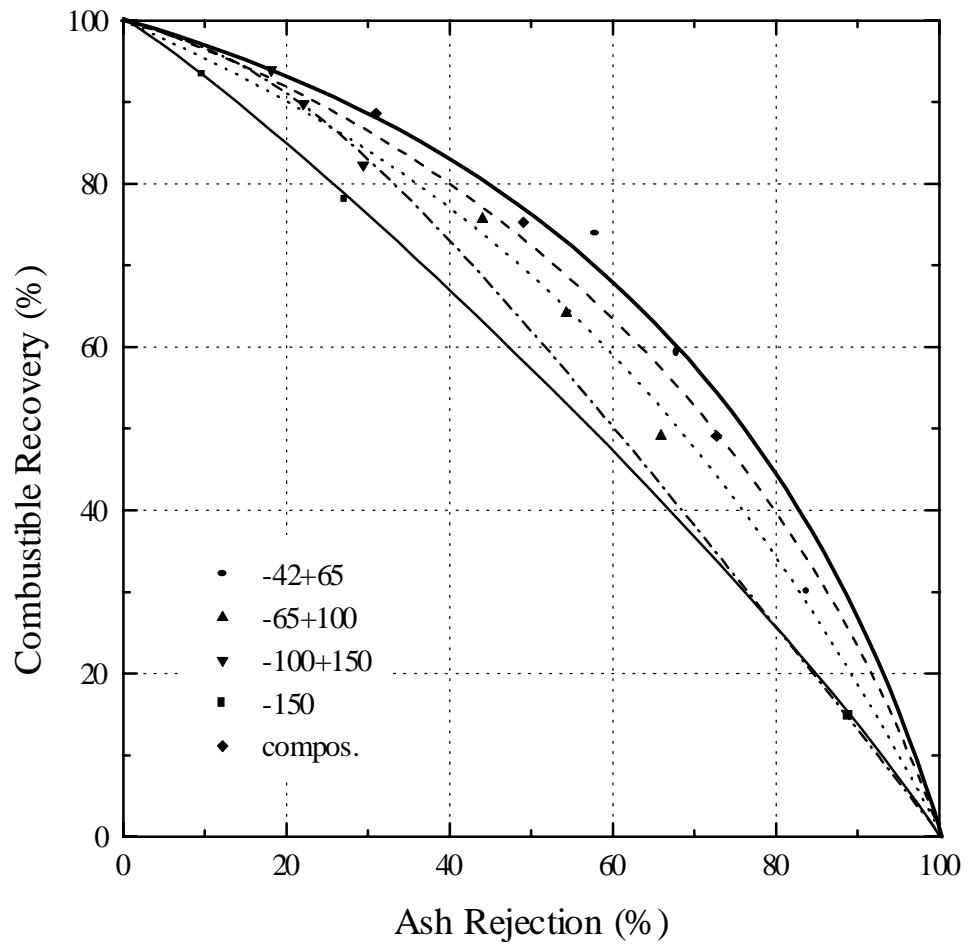


Figure 3.26. The effect of feed size on the separation efficiency of the bench-scale TES unit. The ash rejection vs. recovery curves were obtained on a Sewell Seam sample.

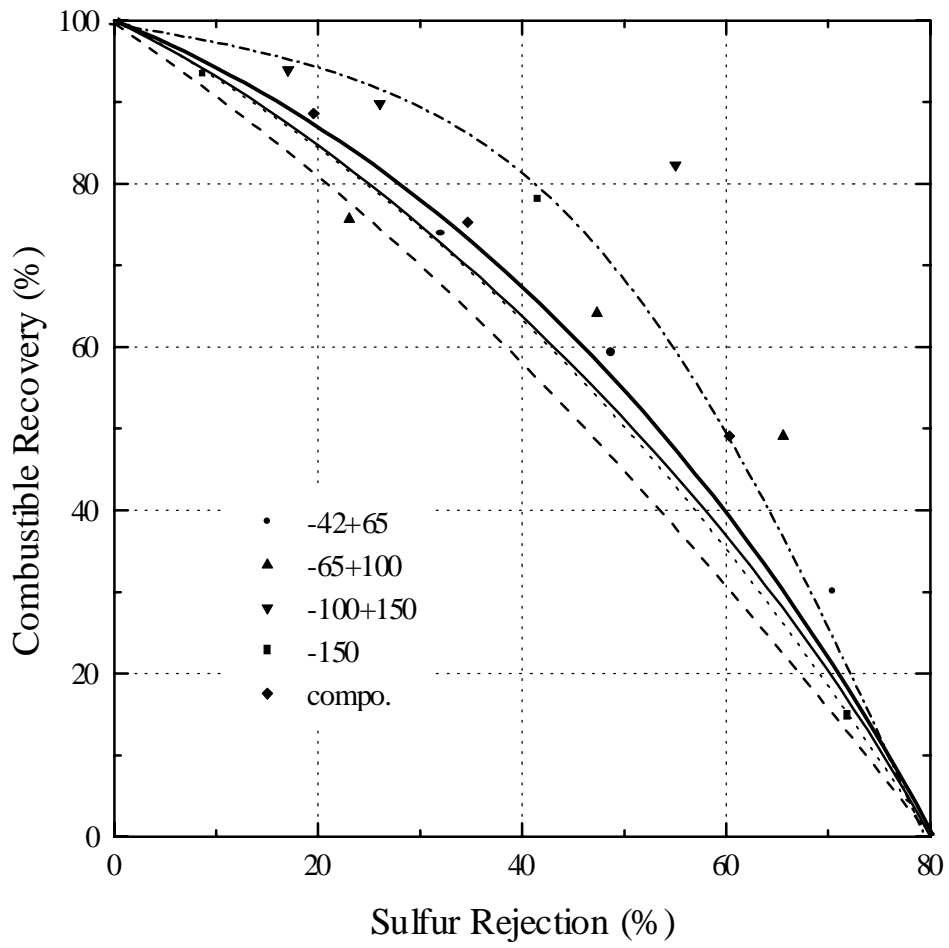


Figure 3.27. The effect of feed size on the separation efficiency of the bench-scale TES unit. The sulfur rejection vs. recovery curves were obtained on a Sewell Seam sample.